

Brushless Permanent Magnet Servomotors

Metin Aydin

*Kocaeli University, Department of Mechatronics Engineering, Kocaeli
Turkey*

1. Introduction

Electrical motors drive a variety of loads in today's world. Almost every industrial process relies on some kind of electrical motors and generators. There exist billions electric motors used in different applications all over the world. Majority of them are small fractional HP motors use in household appliances. However, they used about 5% of the electricity used by the motors. Three phase motors are used in heavier applications and consume substantial amount of electricity. These electric motors operate long hours and consume more than half of the electricity used by motors.

The oldest type of electric motor, wound field DC motor, was the most popular motor for years and easiest for speed control. Although they are replaced by adjustable AC drives in many applications, they are still used in some low power and cost effective applications. The main reason why DC drives faded away over the last decade is that they require converters and maintenance, not to mention their lower torque densities compared to AC motors. Induction motors are also one of the most widely used motors in AC drive applications. They are reliable and don't require maintenance due to the absence of brushes and slip rings. The availability of single phase power is another big plus for these motors. The fact that the rotor windings are present makes the induction motors less efficient and creates cooling problems of the rotor. One crucial drawback of the induction motors is the parameter variation due to the heat caused by the rotor winding.

Variable reluctance motors are also frequently used in the industry and robotics. It's simple and robust stator and rotor structures reduce the cost dramatically compared to other types of motors. The converter requirement is also not very severe. A simple half bridge converter can easily be used to drive the motor. On the other hand, variation of reluctance does also create significant cogging, vibration and audible noise.

As for the synchronous motors, they have benefits and drawbacks of both DC and induction motors. The synchronous motors with field winding can be more efficient than a DC or induction motors and are used in relatively large loads such as generating electricity in power plants. If the rotor winding in synchronous motors is replaced by permanent magnets, another variation of synchronous motors is obtained. These motors are called permanent magnet motors which can be supplied by sinusoidal or trapezoidal currents. These motors have three major types based on their magnet structures as displayed in Fig. 1.

The lack of slip rings and rotor windings as well as high power density, high efficiency and small size make these motors very attractive in the industrial and servo applications. In

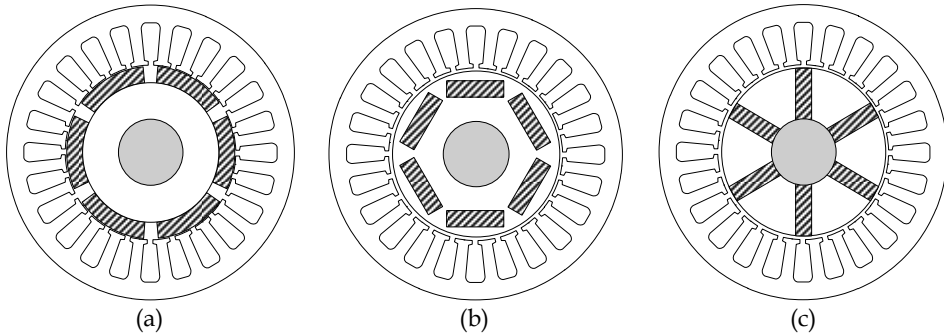


Fig. 1. Surface mounted PM (a), buried PM (b) and spoke type PM (c) motor types

addition, PM servomotors have better torque-speed characteristics and high dynamic response than other motors. Their long operating lives, noise-free operations and high speed ranges are some of the advantages of brushless servomotors.

2. Classification of electric motors

2.1 General motor classification

There are several ways of classifying electric motors by their electrical supply, by rotor structures and stator types. One of the common ways is to categorize them as AC and DC motors as shown in Fig. 2. AC motors use alternating current or voltage as source while DC motors use DC voltage source to supply the windings. DC motors are classified by their field connections such as series, parallel or compound field excitation. AC motors, on the other hand, has two major types: One type is induction motors where rotor magnetic field is generated by electromagnetic induction principles and the other is synchronous motors where the magnetic field is generated by either field winding excitation or permanent magnets. Induction motors could be single or poly-phase and have squirrel-cage or wound rotor. Synchronous motors could have numerous options depending on the rotor type and excitation (Hendershot & Miller, 1995).

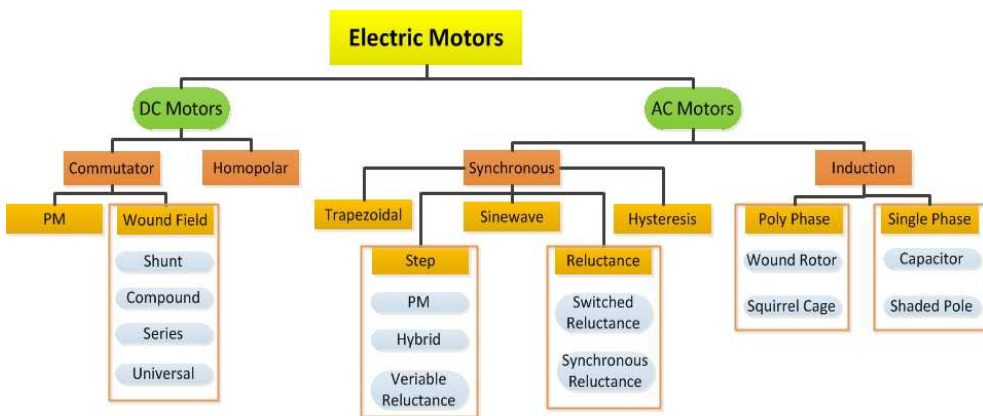


Fig. 2. Fundamental motor classification

Electric motors are also classified by their slots. They are called slotted motors if they do have slots and called non-slotted or slotless motors if they do not have any slot structures. Furthermore, one major classification method is identified by the main flux direction. If the motor has a main flux component which is radial to the shaft, they are called radial flux motors and if the flux component is axial to the motor shaft, then the motors are called axial flux motors where they find various applications because of their structural flexibility.

2.2 Permanent magnet servomotors

There exist various permanent magnet (PM) servomotors in the literature. They can be classified into two main categories, which are surface mounted PM motors where magnets are glued on the rotor surface and buried PM motors where magnets are buried into the rotor.

The use of surface mounted PM motors increases the amount of PM material per pole used in the motor. Using more magnet material usually increases the torque production of the motor while it also increases the motor volume and thus the cost. Buried PM motor and interior PM motor use the flux concentration principles where the magnet flux is concentrated in the rotor core before it gets into the airgap. These motors usually have considerable reluctance torque which arises from the fact that the use of flux concentration in the iron core introduces a position dependent inductance and hence reluctance torque that can be beneficial in certain cases.

PM motors are also classified based on the flux density distribution and the shape of the current excitation. They are listed into two categories, one of which is PM synchronous motors (PMSM) and the other is PM brushless motors (BLDC). PMSM, also called permanent magnet AC (PMAc) motors, has sinusoidal flux density, current and back EMF variation while the BLDC has rectangular shaped flux density, current variation and back EMF. Classification of these two motor types is explained in Table 1.

| | PMSM | BLDC |
|--------------------------|------------|-------------|
| Phase current excitation | Sinusoidal | Trapezoidal |
| Flux density | Sinusoidal | Square |
| Phase back EMF | Sinusoidal | Trapezoidal |
| Power and Torque | Constant | Constant |

Table 1. Classification of permanent magnet motors based on their excitation and back EMF waveforms

| | Surface PM motor | Buried/Interior PM motor |
|-----------------------|----------------------------|------------------------------------|
| Convenience | BLDC | PMSM |
| Flux distribution | Square or Sinusoidal | Usually Sinusoidal |
| Complexity of rotor | Simple | Complex |
| Speed limit | $\sim 1.2 \times \omega_R$ | $\sim 3 \times \omega_R$ or higher |
| High speed capability | Difficult | Possible |
| Control | Relatively easy | More complex |

Table 2. Basic comparison of surface magnet and buried magnet motors



Fig. 3. Typical servomotor (Courtesy of FEMSAN Motor Co.)

Each PM motor type explained has some advantages over another. For instance, surface magnet motor has very simple rotor structure with fairly small speed limits. Buried or interior PM motors have wide speed ranges but their rotor is more complex than both surface magnet and inset PM rotors. In addition, buried or interior PM motors can go up to very high speeds unlike surface magnet motors although their control is more complex than surface magnet type motors. This comparison is also tabulated in Table 2.

2.3 Permanent magnet servomotor structure

A conventional surface mounted PM servomotor structure is illustrated in Fig. 1 (a). The motor has a stator and a PM rotor. The stator structure is slotted and formed by the laminated magnetic steel. A close picture of a laminated stator is shown in Fig. 4. Polyphase windings are placed into the stator slots although a slotless versions of servomotors are also available. The rotor structure is formed by the permanent magnets mounted on the rotor surface, rotor core and shaft. The rotor core is usually laminated. Fig. 5 shows both the stator and the rotor of a typical permanent magnet servomotor with high energy NdFeB magnets.

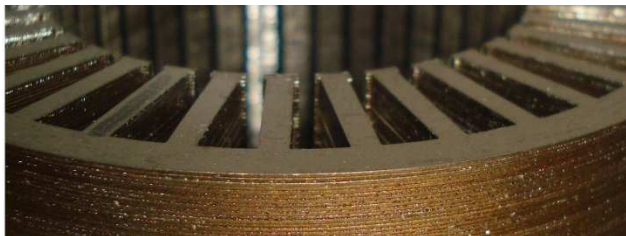


Fig. 4. Stator stack showing the servomotor laminations



Fig. 5. Stator stack showing the motor laminations

2.4 PM servomotor torque-speed and back-EMF characteristics

Fig. 6 shows typical torque-speed characteristics of a brushless PM servomotor. There are two main torque parameters to describe a PM servomotor: Rated torque (T_R) and maximum torque (T_{max}). In addition, there are two major speed points: Rated speed and maximum speed. The region up to rated speed is called constant torque region and the region between the max speed (ω_{max}) and rated speed (ω_R) is called constant power region. During constant torque region, the motor can be loaded up to rated torque usually without any thermal problem. On the other hand, during constant power region, the motor torque starts to drop but the power stays almost constant. Another important characteristic of a PM motor is maximum load point which shows the overload capability of the motor. During this period, the motor can deliver higher torque for a short time to handle cases such as motor overload, start-up etc.

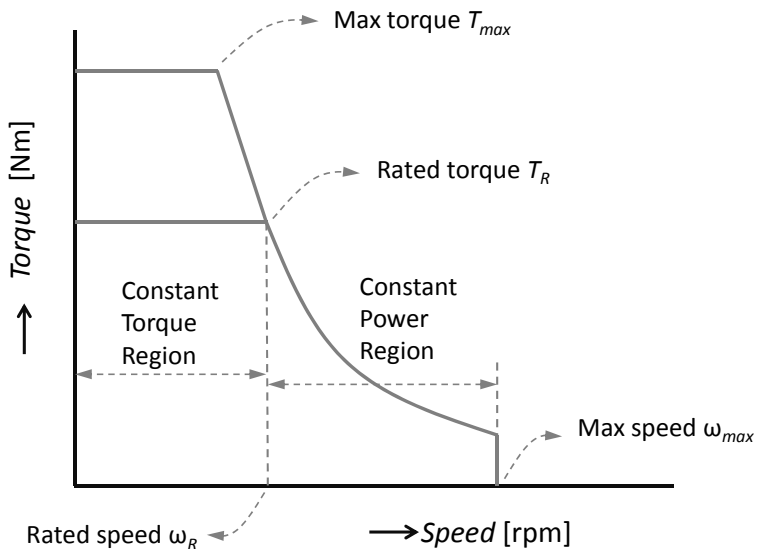


Fig. 6. Torque-speed characteristics of a PM servomotor

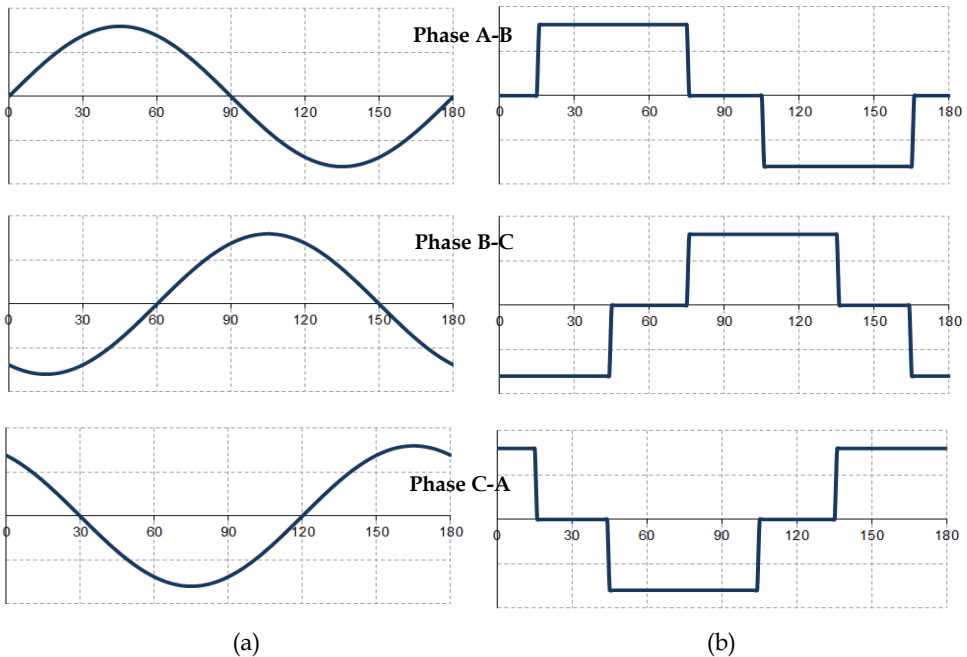


Fig. 7. Trapezoidal (a) and sinusoidal back-EMF (b) waveforms of a PM servomotor

There are two types of PM servomotor alternatives: Sinusoidal and trapezoidal motors. This is made on the basis of back-EMF waveforms. Trapezoidal servomotors have a back-EMF in trapezoidal manner and sinusoidal servomotors have a sinusoidal back-EMF as illustrated in Fig. 7. In addition to back-EMF, the supply current is trapezoidal and sinusoidal in each individual type of motors.

3. Magnetic materials

3.1 Magnetic steel

There exist various electric steel materials used in servomotors. Material type and grade depends mainly on the application and cost. High quality materials with high saturation and low loss levels are used in high performance and high speed applications while thick and high loss materials are used in low speed and cost effective applications. Non-oriented electrical steels are usually used in electric motor applications. Low magnetic loss and high permeability characteristics are valuable for applications where energy efficient, low loss, low noise and small size are important. One of the most frequently used magnetic steel lamination material is M270-35A (similar to M19 in the US). This material or similar grade is used in most PM servomotor applications. If high saturation levels and low losses at high speeds are required, materials such as Vacoflux50 would be a good option. The BH curve of these materials in addition to materials with high loss and thin high saturation level are all displayed in Fig. 8. Moreover, Table 3 shows the electrical and mechanical properties of various non-oriented electrical steel materials used in different motor applications.

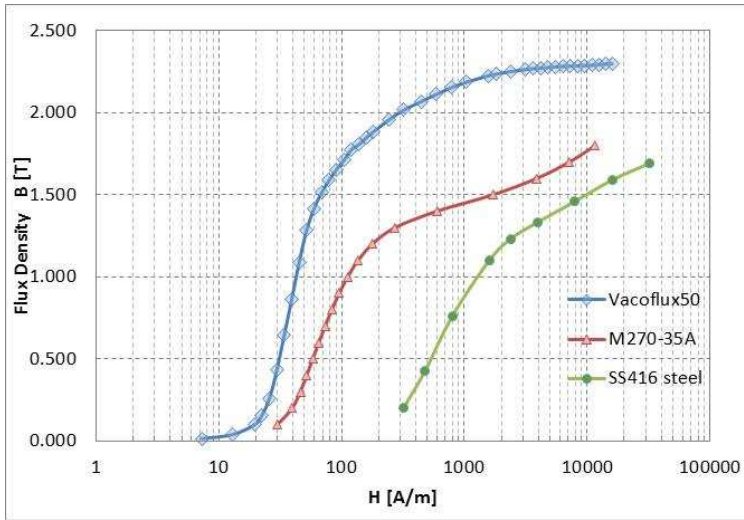


Fig. 8. Examples of steel materials with magnetic and structural properties

| Grade EN 10106 | Thickness mm | Maximum specific total loss at 50 Hz $\hat{J} = 1.5 T$ | | Minimum magnetic polarization at 50 Hz $\hat{H} = 2500$ | | | Grade EN 10106 | Conventional density kg/dm ³ | Resistivity $\mu\Omega\text{cm}$ | Yield strength N/mm ² | Tensile strength N/mm ² | Young's Modulus (E) RD N/mm ² | TD N/mm ² | Hardness HV5 (V/PN) |
|----------------|--------------|--|--------------|---|--------|-------------|----------------|---|----------------------------------|----------------------------------|------------------------------------|--|----------------------|---------------------|
| | | W/kg | 1.0 T** W/kg | T | 5000 T | 10000 A/m T | | | | | | | | |
| M235-35A | 0.35 | 2.35 | 0.95 | 1.49 | 1.60 | 1.70 | M235-35A | 7.60 | 59 | 460 | 580 | 185 000 | 200 000 | 220 |
| M250-35A | 0.35 | 2.50 | 1.00 | 1.49 | 1.60 | 1.70 | M250-35A | 7.60 | 55 | 455 | 575 | 185 000 | 200 000 | 215 |
| M270-35A | 0.35 | 2.70 | 1.10 | 1.49 | 1.60 | 1.70 | M270-35A | 7.65 | 52 | 450 | 565 | 185 000 | 200 000 | 215 |
| M300-35A | 0.35 | 3.00 | 1.20 | 1.49 | 1.60 | 1.70 | M300-35A | 7.65 | 50 | 370 | 490 | 185 000 | 200 000 | 185 |
| M330-35A | 0.35 | 3.30 | 1.30 | 1.49 | 1.60 | 1.70 | M330-35A | 7.65 | 44 | 300 | 430 | 200 000 | 220 000 | 150 |
| M700-35A* | 0.35 | 7.00 | 3.00 | 1.60 | 1.69 | 1.77 | M700-35A* | 7.80 | 30 | 290 | 405 | 210 000 | 220 000 | 125 |
| M250-50A | 0.50 | 2.50 | 1.05 | 1.49 | 1.60 | 1.70 | M250-50A | 7.60 | 59 | 475 | 590 | 175 000 | 190 000 | 220 |
| M270-50A | 0.50 | 2.70 | 1.10 | 1.49 | 1.60 | 1.70 | M270-50A | 7.60 | 55 | 470 | 585 | 175 000 | 190 000 | 220 |
| M290-50A | 0.50 | 2.90 | 1.15 | 1.49 | 1.60 | 1.70 | M290-50A | 7.60 | 55 | 465 | 580 | 185 000 | 200 000 | 220 |
| M310-50A | 0.50 | 3.10 | 1.25 | 1.49 | 1.60 | 1.70 | M310-50A | 7.65 | 52 | 385 | 500 | 185 000 | 200 000 | 190 |
| M330-50A | 0.50 | 3.30 | 1.35 | 1.49 | 1.60 | 1.70 | M330-50A | 7.65 | 50 | 375 | 495 | 185 000 | 200 000 | 185 |
| M350-50A | 0.50 | 3.50 | 1.50 | 1.50 | 1.60 | 1.70 | M350-50A | 7.65 | 44 | 305 | 450 | 200 000 | 210 000 | 165 |
| M400-50A | 0.50 | 4.00 | 1.70 | 1.53 | 1.63 | 1.73 | M400-50A | 7.70 | 42 | 305 | 445 | 200 000 | 210 000 | 160 |
| M470-50A | 0.50 | 4.70 | 2.00 | 1.54 | 1.64 | 1.74 | M470-50A | 7.70 | 39 | 300 | 435 | 200 000 | 210 000 | 155 |
| M530-50A | 0.50 | 5.30 | 2.30 | 1.56 | 1.65 | 1.75 | M530-50A | 7.70 | 36 | 295 | 430 | 200 000 | 210 000 | 150 |
| M600-50A | 0.50 | 6.00 | 2.60 | 1.57 | 1.66 | 1.76 | M600-50A | 7.75 | 30 | 285 | 405 | 210 000 | 220 000 | 125 |
| M700-50A | 0.50 | 7.00 | 3.00 | 1.60 | 1.69 | 1.77 | M700-50A | 7.80 | 25 | 285 | 405 | 210 000 | 220 000 | 125 |
| M800-50A | 0.50 | 8.00 | 3.60 | 1.60 | 1.70 | 1.78 | M800-50A | 7.80 | 23 | 300 | 415 | 210 000 | 220 000 | 130 |
| M940-50A | 0.50 | 9.40 | 4.20 | 1.62 | 1.72 | 1.81 | M940-50A | 7.85 | 18 | 300 | 415 | 210 000 | 220 000 | 130 |
| M310-65A | 0.65 | 3.10 | 1.25 | 1.49 | 1.60 | 1.70 | M310-65A | 7.60 | 59 | 465 | 590 | 175 000 | 190 000 | 220 |
| M330-65A | 0.65 | 3.30 | 1.35 | 1.49 | 1.60 | 1.70 | M330-65A | 7.60 | 55 | 460 | 585 | 185 000 | 205 000 | 220 |
| M350-65A | 0.65 | 3.50 | 1.50 | 1.49 | 1.60 | 1.70 | M350-65A | 7.60 | 52 | 375 | 490 | 185 000 | 205 000 | 185 |
| M400-65A | 0.65 | 4.00 | 1.70 | 1.52 | 1.62 | 1.72 | M400-65A | 7.65 | 44 | 310 | 450 | 185 000 | 205 000 | 165 |
| M470-65A | 0.65 | 4.70 | 2.00 | 1.53 | 1.63 | 1.73 | M470-65A | 7.65 | 42 | 305 | 445 | 185 000 | 205 000 | 160 |
| M530-65A | 0.65 | 5.30 | 2.30 | 1.54 | 1.64 | 1.74 | M530-65A | 7.70 | 39 | 300 | 425 | 190 000 | 210 000 | 145 |
| M600-65A | 0.65 | 6.00 | 2.60 | 1.56 | 1.66 | 1.76 | M600-65A | 7.75 | 36 | 300 | 420 | 190 000 | 210 000 | 140 |
| M700-65A | 0.65 | 7.00 | 3.00 | 1.57 | 1.67 | 1.76 | M700-65A | 7.75 | 30 | 290 | 395 | 210 000 | 220 000 | 125 |
| M800-65A | 0.65 | 8.00 | 3.60 | 1.60 | 1.70 | 1.78 | M800-65A | 7.80 | 25 | 300 | 405 | 210 000 | 220 000 | 130 |
| M1000-65A | 0.65 | 10.00 | 4.40 | 1.61 | 1.71 | 1.80 | M1000-65A | 7.80 | 18 | 295 | 400 | 210 000 | 220 000 | 125 |

Table 3. Non-oriented electric steel material properties (Source: Cogent)

3.2 Permanent magnets

Permanent magnet materials have been used in electric motors for decades. One important property of permanent magnets is the maximum energy product (*MEP*) which is the multiplication of residual flux density (*B_r*) and coercive force (*H_c*). In other words, *MEP* represents the maximum energy available per unit volume (kJ/m³). *MEP* is also an indication of magnet force. Furthermore, the larger the *MEP*, the smaller the magnet material needed for the same force. Permeability is another important property of the

magnets. It is the slope of the demagnetization curve in the linear region. Small permeability means high flux levels before the magnet is irreversibly demagnetized.

Alnico magnets which are Aluminum, nickel, iron and later addition of cobalt based materials was one of the important discoveries in permanent magnet technology and is still widely used today. These magnets can be magnetized in any direction by simply heating the magnet and cooling them in a magnetic field to give a preferred magnetic direction. Traditionally, Alnico magnets were largely used in PM motors. One advantage of Alnico magnets is that they have a high residual flux density (B_r). They have excellent temperature stability and strong corrosion resistance level. Their working temperatures can go up to 500 degrees. However, they can be demagnetized very easily. In addition, the maximum energy product of these magnets is not very high.

Ferrite magnets, also called ceramic magnets, are one of the cheapest magnets manufactured in industry. They have very high intrinsic coercive force (H_{ci}) and therefore, they are very difficult to demagnetize. They can easily be magnetized in a variety of formats. The raw material is so abundant that it is found in numerous applications. This kind of magnet material has a good resistance to corrosion and can operate at high temperatures up to 300 degrees. These materials are used even today for applications where space and cost are not important requirements.

Rare-earth magnets are strong permanent magnets made from the alloys elements such as Neodymium and Samarium. Discovery of these strong magnets have changed the future of permanent magnet motor technology as well as servomotors and the magnetic field can be increased to 1.5T levels. There are two types of rare-earth magnets available: Neodymium magnets and Samarium cobalt magnets.

The first generation rare earth magnets use Samarium and Cobalt (SmCo). One of the biggest advantages of such magnets is that they provide very high MEP compared to Alnicos and Ferrites. This big improvement in high MEP is made possible by the high coercive force. Nonetheless, they are very brittle and both the raw material cost and the production cost are quite high compared to other types of magnets. The revolution of rare earth magnets accelerated with the discovery of Neodymium Iron-Boron (NdFeB) magnets with even higher MEP in 1982. NdFeB magnets are produced by pressing powders in a magnetic field and their energy products can go up to 420 kJ/m³. This material is much stronger than SmCo and the cost is much lower simply because they are composed of mostly iron which is much cheaper than cobalt. However, they have to be protected against corrosion and their working temperature is also lower compared to SmCo magnets.

A brief comparison of different magnets used in PM motors is illustrated in Table 4. The rare earth magnets are the most common magnet materials used in PM servomotors and the table clearly shows significant benefits of such magnets. NdFeB magnets have higher flux density levels up to 1.5T and higher MEPs but their working temperature is lower (up to 200 °C).

| Materials | B_r [T] | H_c [kA/m] | BH_{max} [kJ/m ³] | T_c [°C] | T_{w-max} [°C] |
|-----------|-----------|--------------|---------------------------------|------------|------------------|
| Alnico | 1.2 | 10 | 6 | 500 | 500 |
| Ferrite | 0.43 | 10 | 5 | 300 | 300 |
| SmCo | Up to 1.1 | Up to 820 | Up to 240 | Up to 820 | Up to 350 |
| NdFeB | Up to 1.5 | Up to 1033 | Up to 422 | Up to 380 | Up to 200 |

Table 4. Typical permanent magnet material magnetic properties

NdFeB magnets are more common rare earth magnets than SmCo, cheaper but more brittle. SmCo magnets are widely used in applications in which higher operating temperature and higher corrosion and oxidation resistance are crucial. A basic comparison of the four major types of permanent magnet materials used in motors today is illustrated in Fig. 9.

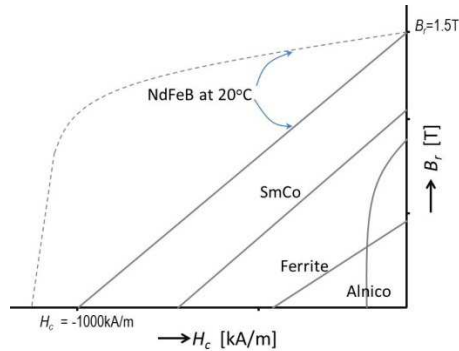


Fig. 9. Flux density versus magnetizing field for the important magnets classes

4. Basic permanent magnet motor design process

Design procedure for any PM servomotor is shown in Fig. 10. This process comprises three main steps: Electromagnetic, structural and thermal designs. Electromagnetic design starts with magnetic circuit modeling and parameter optimization with a given set of design specifications. A series of optimizations such as pole number, loading, current density, dimensional limits etc. have to be performed to find the optimum parameters of the motor before proceeding further. When a design is obtained that meets the technical spec, a quick motor simulation and the influence of parameter variation must be carried out using simulation software such as SPEED (PC-BDC Manual, 2002). A detailed electromagnetic finite element analysis (FEA) either in 2D or 3D is the next step to verify that the design meets the specified torque-speed characteristics and performance. After an electromagnetic design is finalized, structural and thermal analyses (MotorCAD Manual 2004) have to be completed. It should be pointed out that structural analysis is not a necessity at low speed servomotor designs. If the motor does not meet the structural or thermal tests, then the electromagnetic design study should be repeated for a better design. A motor design has to be finalized after a design passes all of the main steps (Aydin et al. 2006).

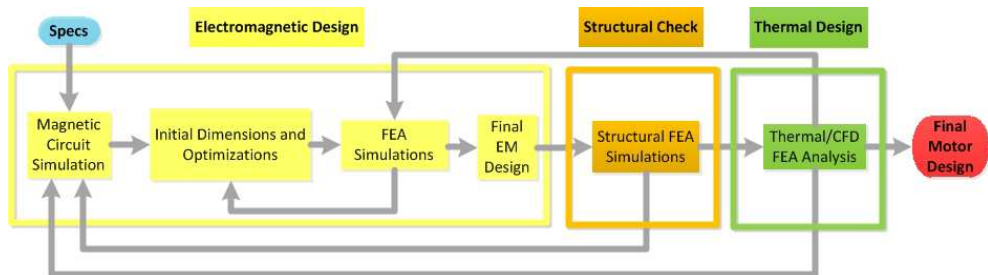


Fig. 10. PM servomotor design process

5. Dynamic model of PM servomotors

Following assumptions are made for the analysis of PM servomotors: The inverter is ideal with no losses; no DC voltage ripple exists in the DC link; the supply current is sinusoidal and no saturation is considered; eddy current and hysteresis losses are negligible; and all motor parameters are constant. Based on these assumptions, permanent magnet servomotor dynamic equations in the synchronous rotating reference frame are written as

$$v_q = r_s i_q + L_q \frac{di_q}{dt} - \omega_e L_d i_d + \omega_e \lambda_f \tag{1}$$

$$v_d = r_s i_d + L_d \frac{di_d}{dt} - \omega_e L_q i_q \tag{2}$$

$$T_m = \frac{3P}{2} \left[\lambda_f i_q + (L_d - L_q) i_d i_q \right] \tag{3}$$

where v_d and v_q are d and q axis voltages, i_d and i_q are d and q-axis currents, r_s is stator resistance, L_d and L_q are d-q axis inductances, ω_e is synchronous speed, λ_f is magnet flux linkage, P is pole number and T_m is the electromagnetic torque of the motor. During constant flux operation, i_d becomes zero and the torque equation becomes

$$T_m = \frac{3P}{2} \lambda_f i_q = K_T i_q \tag{4}$$

where K_T is the torque constant of the motor. This equation becomes similar to standard DC motor and therefore provides ease of control. The torque dynamic equation is

$$T_m = T_L + B\omega_m + J \frac{d\omega_m}{dt} \tag{5}$$

equivalent circuit of the steady-state operation of the PM servomotors in d-q reference model is shown in Fig. 11. Independent control of both q-axis and d-axis components of the currents is possible with the vector controlled PM servomotors. Both voltage controlled and current controlled inverters are possible to drive the motor.

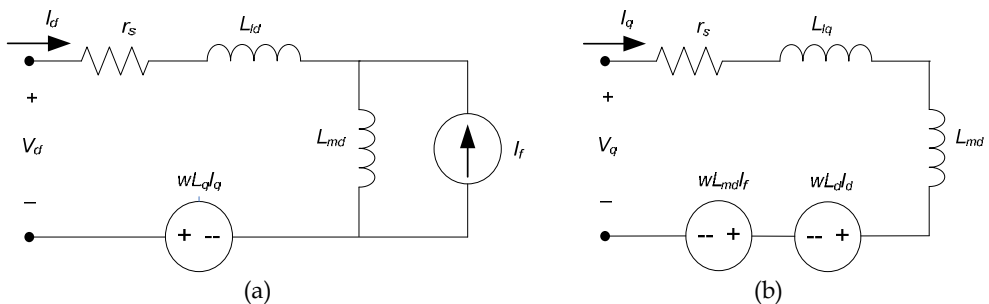


Fig. 11. Equivalent circuit of PM servomotors (a) d-axis equivalent circuit and (b) q-axis equivalent circuit

6. Use of finite element analysis in PM servomotors

The finite element method (FEM) is a numerical method for solving the complex electromagnetic field problems and circuit parameters. It is specifically convenient for problems with non-linear material characteristics where mathematical modeling of the system would be difficult. This method involves dividing the servomotor cross section or volume into smaller areas or volumes. It could be 2D objects in the case of 2D FEM analysis or 3D objects in the case of 3D analysis. The variation of the magnetic potential throughout the motor is expressed by non-linear differential equations in finite element analysis. These differential equations are derived from Maxwell equations and written in terms of vector potential where the important field quantities such as flux, flux direction and flux density can be determined.

The FEM can accurately analyze the magnetic systems which involve permanent magnets of any shape and material. There is no need to calculate the inductances, reluctances and torque values using circuit type analytical methods because these values can simply be extracted from the finite element analysis. Another important advantage of using FEM over analytical approach is the ability to calculate the torque variations or torque components such as cogging torque, ripple torque, pulsating torque and average torque accurately without too much effort.

There are various FEA packages used for motor analysis. FEA packages have 3 main mechanisms which are pre-processor, field solver and post-processor. Model creation, material assignments and boundary condition set-up are all completed in the pre-processor part of the software. Field solver part has 4 main steps to solve the numerical problems. After the pre-process, the software generates the mesh, which is the most important part of getting accurate results. User's experience in generating the mesh has also an important effect on the accuracy of the results. Then, the FEA package computes the magnetic field, performs some analysis such as flux, torque, force and inductance, and checks if the error criteria have been met. If not, it refines the mesh and follows the same steps based on the user's inputs until it reaches the specified error limit. This procedure is shown in Fig. 12. In the post-processor, magnetic field quantities are displayed and some quantities such as force, torque, flux, inductance etc. are all calculated.

7. Torque quality

Permanent magnet servomotors are widely used in many industrial applications for their small size, higher efficiency, noise-free operation, high speed range and better control. This makes quality of their torque an important issue in wide range of applications including servo applications. For example, servomotors used in defense applications, robotics, servo systems, electric vehicles all require smooth torque operation.

One of the most important issues in PM servomotors is the pulsating torque component which is inherent in motor design. If a quality work is not completed during the design stage, this component can lead to mechanical vibrations, acoustic noise, shorter life and drive system problems. In addition, if precautions are not taken, it can lead to serious control issues especially at low speeds. Minimization of the pulsating torque components is of great importance in the design of permanent magnet servomotors.

In general, calculation of torque quality is a demanding task since the torque quality calculation does not only consider the torque density of the motor but also consider the

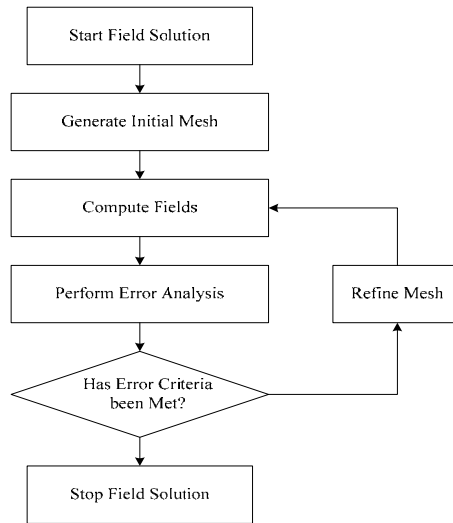


Fig. 12. General procedure for any commercially available FEA software

pulsating torque component. Therefore, a mathematical approach about torque quality should include harmonic analysis of electric drive system rather than a simple sizing of the motor.

Output torque of a PM servomotor has an average torque and pulsating torque components. The pulsating torque consists of cogging torque and ripple torque components. Cogging torque occurs from the magnetic permeance variation of the stator teeth and the slots above the permanent magnets. Presence of cogging torque is a major concern in the design of PM motors simply because it enhances undesirable harmonics to the pulsating torque. Ripple torque, on the other hand, occurs as a result of variations of the field distribution and the stator MMF. At high speed operations, ripple torque is usually filtered out by the inertia of the load or system. However, at low speeds 'torque-ripple' produces noticeable effects on the motor shaft that may not be tolerable in smooth torque and constant speed applications. Servomotors can also be categorized by the shape of their back EMF waveforms which can take different forms such as sinusoidal and trapezoidal as seen in Fig. 13. Any non-ideal

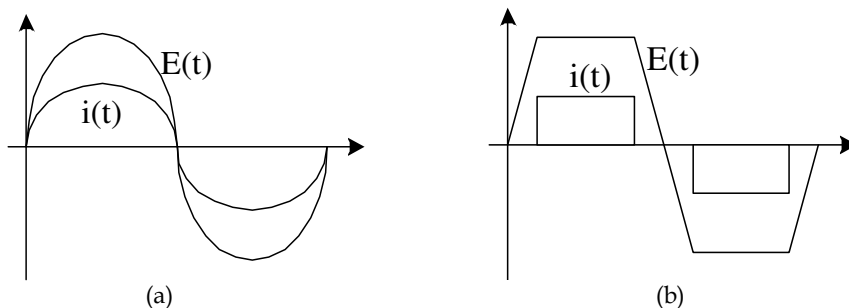


Fig. 13. Current and back EMF waveform options in PM servomotors: (a) sinusoidal back-EMF and current and (b) trapezoidal back-EMF and current

situations such as converter caused disturbed stator current waveform and disturbed back EMF waveform arising from the design cause non-sinusoidal current and airgap flux density waveforms which result in undesired pulsating torque components at the motor output. In other words, if the airgap flux density waveform is disturbed, pulsating torque at the motor shaft becomes inevitable (Jahns & Soong, 1996).

7.1 Electromagnetic torque in PM motors

Definitions of the torque components will be given before getting into the subject any deeper. First, "cogging torque" is defined as the pulsating torque component produced by the variation of the airgap permeance or reluctance of the stator teeth and slots above the magnets as the rotor rotates. In other words, there is no stator excitation involved in cogging torque production of a PM motor. Second, "ripple torque" is the pulsating torque component generated by the stator MMF and rotor MMF. Ripple torque is mainly due to the fluctuations of the field distribution and the stator MMF which depends on the motor structure and the current waveform. This component can take two forms, one of which resulting from the MMF created by the stator windings and the other from MMF created by the rotor magnets. The second form is the torque created by stator MMF and rotor magnetic reluctance variation. In surface mounted PM servomotor, since there exists no rotor reluctance variation, there is no second form of the ripple torque and the ripple torque is mainly created by the first form. The third definition is "pulsating torque" which is defined as the sum of both cogging and ripple torque components (Sebastian et al., 1986 and Ree & Boules, 1989).

In the following analysis, it is assumed that a Y connected three phase unsaturated PM motor used and it has a constant airgap length and symmetrical stator winding. It is also assumed that stator currents contain only odd harmonics and current harmonics of the order of three does not exist. Finally, armature reaction is assumed negligible. For PM motors, at instant t , the instantaneous electromagnetic torque produced by phase A can be written as the interaction of the magnetic field and the phase current circulating in N turns

$$T_a(t) = 2pNi_a(t) \int_{-\pi/2mp}^{\pi/2mp} R_g L_e B(\theta_r, t) d\theta_r \quad (6)$$

where R_g is airgap radius of the servomotor, L_e is effective stack length, p is pole pairs and m is the number of phases.

The back-EMF of the motor induced in phase A at the time instant t is given by

$$e_a(t) = 2pN \int_{-\pi/2mp}^{\pi/2mp} R_{mean} L_R B(\theta_r, t) \omega_m d\theta_r \quad (7)$$

where ω_m is the rotor angular speed. The back-EMF in phase a can also be written as

$$e_a(t) = \omega_m 2pN \int_{-\pi/2mp}^{\pi/2mp} R_{mean} L_R B(\theta_r, t) d\theta_r \quad (8)$$

Substituting (8) into (6), the torque expression becomes

$$T_a(t) = \frac{e_a(t) \cdot i_a(t)}{\omega_m} \quad (9)$$

For the Y-connected three-phase stator winding, the back-EMF in phase *A* can be written as the summation of odd harmonics including fundamental component:

$$e_a = E_1 \sin \omega t + E_3 \sin 3\omega t + E_5 \sin 5\omega t + E_7 \sin 7\omega t + \dots \quad (10)$$

and likewise the current in phase *A* can be written as

$$i_a = I_1 \sin \omega t + I_5 \sin 5\omega t + I_7 \sin 7\omega t + I_{11} \sin 11\omega t + I_{13} \sin 13\omega t + \dots \quad (11)$$

where E_n is the n^{th} time harmonic peak value of the back EMF, which is produced by n^{th} space harmonic of the airgap magnetic flux density B_{gn} and I_n is the n^{th} time harmonic peak value of current.

The product of back-EMF and current $e_a i_a$ is composed of an average component and even-order harmonics for all phases. The total instantaneous torque contributed by each motor phase is proportional to the product of back EMF and phase current. In other words, the total instantaneous torque is the sum of the torques produced by phase *a*, *b*, and *c* and given by,

$$T_m(t) = \frac{1}{\omega_m} [e_a(t) i_a(t) + e_b(t) i_b(t) + e_c(t) i_c(t)] \quad (12)$$

Since the phase shifts between $e_a i_a$ and $e_b i_b$ and between $e_a i_a$ and $e_c i_c$ are $-2\pi/3$ and $2\pi/3$, respectively, the sum ($e_a i_a + e_b i_b + e_c i_c$) will contain an average torque component and harmonics of the order of six. The other harmonics are all eliminated. Thus, the final instantaneous electromagnetic torque equation of a servomotor can be written as

$$T_m(t) = T_0 + \sum_{n=1}^{\infty} T_{6n} \cos n6\omega t \quad (13)$$

where T_0 is the average torque, T_{6n} is harmonic torque components and $n = 1, 2, 3, \dots$. In the ideal case, if the back-EMF's and the armature currents are sinusoidal, then the electromagnetic torque is constant and no ripple torque exists as illustrated in Fig. 14. The same quantities are plotted for sinusoidal back EMF and square or trapezoidal stator current waveforms and the presence of the pulsating torque component is observed clearly. The resultant plots including torque pulsations for all cases are shown in Fig. 14.

7.2 Cogging torque

7.2.1 Cogging torque theory

Existence of cogging torque is always a cause of concern in the design of PM servomotors. It in fact demonstrates the quality of a servomotor. This torque component is often desired that the motor produces a smooth torque in a wide speed range. Cogging torque adds unwanted harmonic components to both torque output and the torque-angle curve, which results in torque pulsation. This produces vibration and noise, both of which may be amplified in variable speed drive when the torque frequency coincides with a mechanical resonant frequency of the stator and rotor. In addition, if rotor positioning is required at very low speeds, the elimination of cogging torque component becomes even more crucial and must be eliminated completely during the design stage (Li & Slemmon, 1988).

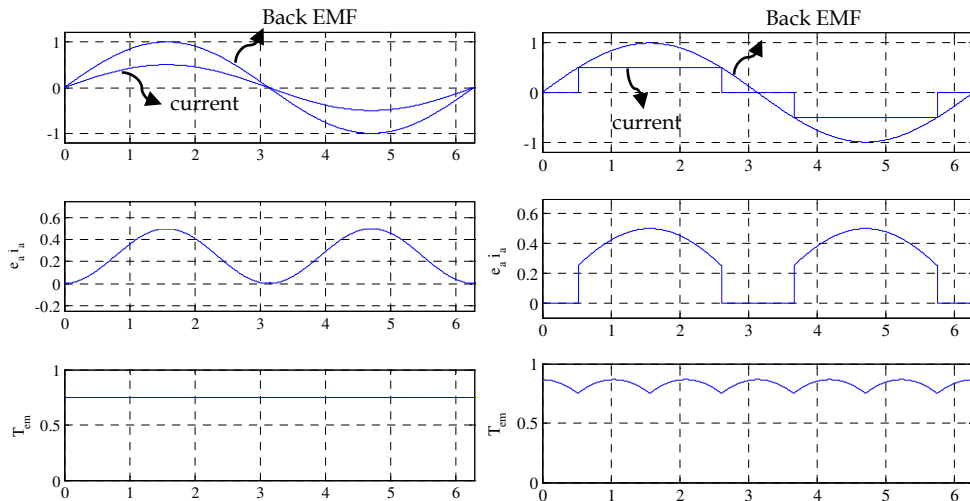


Fig. 14. Torque output for current and back EMF waveforms as a function of electrical cycle
Cogging torque is sensitive to varying rotor position and can be expressed by

$$T_{\text{cog}}(\theta_r) = -\frac{1}{2} \phi_g^2 \frac{dR_g}{d\theta_r} \quad (14)$$

where ϕ_g is the airgap flux, R is the reluctance of the airgap and θ_r is the rotor position. Cogging torque increases due to the increased airgap flux as the magnet strength is increased. Nevertheless, the cogging torque results from the non-uniform flux density in the airgap. As the stator teeth become saturated, the flux begins to distribute evenly in the motor airgap and the cogging torque decreases.

In addition, if there is no airgap reluctance variation as in slotless motors, no cogging component occurs. For a slotted stator configuration, the airgap permeance or reluctance is non-uniform because of the shape of the stator, saturation of the lamination material, slot openings and the space between the rotor magnets. This non-uniform reluctance or magnetic flux path causes the airgap flux density to vary with rotor position. This results in cogging torque, and generates vibration.

7.2.2 Minimization of cogging torque component

Cogging torque minimization is a significant concern during the design of brushless PM servomotors, and it is one of the main sources of torque and speed fluctuations especially at low speeds and load with low inertias. A variety of techniques are available for reducing the cogging torque of conventional PM servomotors, such as skewing the slots, shaping or skewing the magnets, displacing or shifting magnets, employing dummy slots or teeth, optimizing the magnet pole-arc, employing a fractional number of slots per pole, and imparting a sinusoidal self-shielding magnetization distribution. A summary of these methods are displayed in Fig. 15 (Bianchi & Bolognani, 2002).

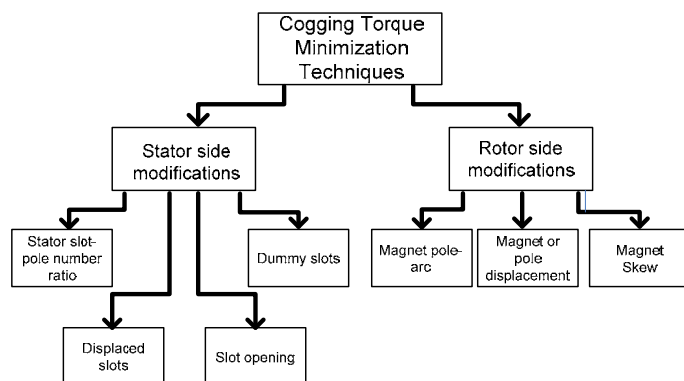


Fig. 15. Summary of cogging torque minimization techniques for PM servomotors

Minimization of cogging torque in PM servomotors can be accomplished by modifications either from stator side or from rotor side. Choosing the appropriate “ratio of stator slot number to rotor pole number” combination is one of the common ways to minimize cogging torque component. This is a design based choice and is the most common method to minimize the unwanted cogging torque components in PM servomotors. Utilizing dummy slots in stator teeth increases the frequency of cogging and reduces its amplitude. Similarly, “displaced slots and slot openings” is a different method to minimize cogging component. In integral slot servomotors ($q=1$ slots/pole/phase), each rotor magnet has the same position relative to the stator slots resulting in cogging torque components which are all in phase, leading to a high resultant cogging torque. Nevertheless, in fractional slot servomotors, where $q \neq 1$ slots/pole/phase rotor magnets have different positions relative to the stator slots generating cogging torque components which are out of phase with each other. The resultant cogging torque is, thus, reduced since some of the cogging components are partially cancelled out. Even uncommon combinations such as 33, 39 or 45 slots are employed for certain applications to obtain small cogging torque components even though it generates an unbalanced servomotor.

Rotor side cogging torque minimization techniques are more cost effective compared to stator side methods and classified into three different categories: variable or constant magnet pole-arc to pole-pitch ratio, pole displacement and magnet skew. Techniques applied to rotor structure are simpler and less costly than stator side techniques. One of the most effective techniques used in servomotors is to employ an appropriate magnet pole-arc to pole-pitch ratio. Reducing the magnet pole-arc to pole-pitch ratio reduces the magnet leakage flux, but it also reduces the magnet flux, and, consequently, the average torque. Another method of reducing the cogging torque is to employ variable magnet pole-arcs for adjacent magnets such that the phase difference between the associated cogging torques results in a smaller net cogging.

7.2.3 Predicting cogging torque using FEA

Finite element analysis (FEA) can correctly examine the PM servomotors. The motor designers do not need to go through cumbersome circuit type analytical methods because important parameters such as flux, inductance, force and torque can simply and accurately

be extracted from the finite element analysis. Even cogging torque component can precisely be calculated using modern FEA software.

Flux 2D software package by Cedrat Co., which is one of the frequently used FEA software in academia and industry, is used in the analyses of the PM servomotor given in Fig. 16 - Fig. 18 (Flux 2D and 3D Tutorial 2002). Cogging torque is obtained using no-load simulations. Rotor structure is rotated for one slot pitch and torque values are calculated using the Flux 2D. Fig. 16 shows both no-load flux density distribution of a 24 slot-8 pole PM servomotor as well as its cogging torque variation over one slot-pitch. Fig. 17 displays the rotor a disc type PM servomotor, its FEA predicted and experimentally verified cogging torque variation. The results show that FEA work well for the cogging torque predictions.

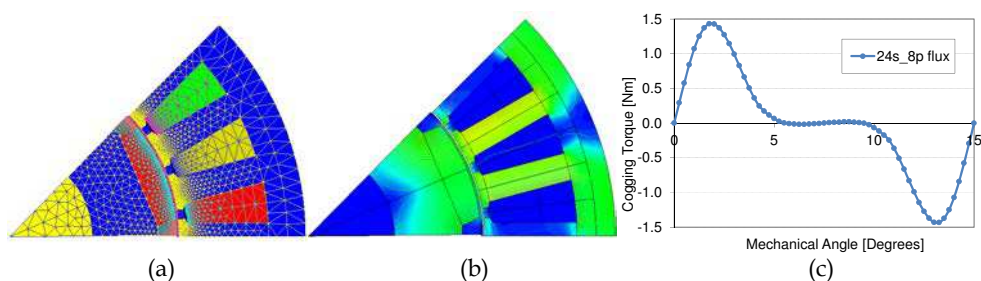


Fig. 16. 2D-FE Model of 24 slots with 8 poles servomotor (a) mesh structure, (b) flux density distribution and (c) cogging torque variation

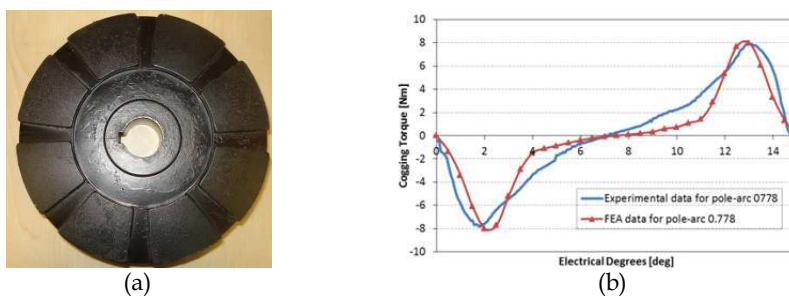


Fig. 17. Rotor structure of a disc type PM servomotor (a), prediction of cogging torque with FEA and experimental data (b)

7.3 Torque ripple

Torque ripple is another important undesired torque element in PM servomotors. It occurs as a result of fluctuations of the field distribution and the stator MMF. In other words, torque ripple depends on the MMF distribution and its harmonics as well as the magnet flux distribution. At high speeds, torque ripple is usually filtered out by the system inertia. However, at low speeds torque-ripple may produces noticeable effects on motor shaft that may not be tolerable in smooth torque and constant speed servo applications.

Fig. 18 shows an interior permanent magnet (IPM) servomotor geometry, flux lines and flux density distribution at no load operation. If the motor is supplied by a harmonic free

excitation, almost no ripple exists at the motor output (Fig. 19). However, if inverter or motor driven harmonics, such as integer slot motors or single segmented rotors with $q=1$ with no skew, exist in the current excitation, significant torque ripple appears at the motor output and precautions must be taken to lower this component as much as possible. One of common techniques to reduce the torque ripple component and obtain smooth torque output is to use segmented rotor. In order to use this approach, rotor is divided into segments and each piece is rotated with respect to each other to obtain ripple free output. As displayed in Fig. 19, if no segment is used, more than 130% of torque ripple is observed at the motor output. When the rotor is divided into 4 segments, torque ripple is reduced to less than 6% of the average torque which is a reasonable number for most applications.

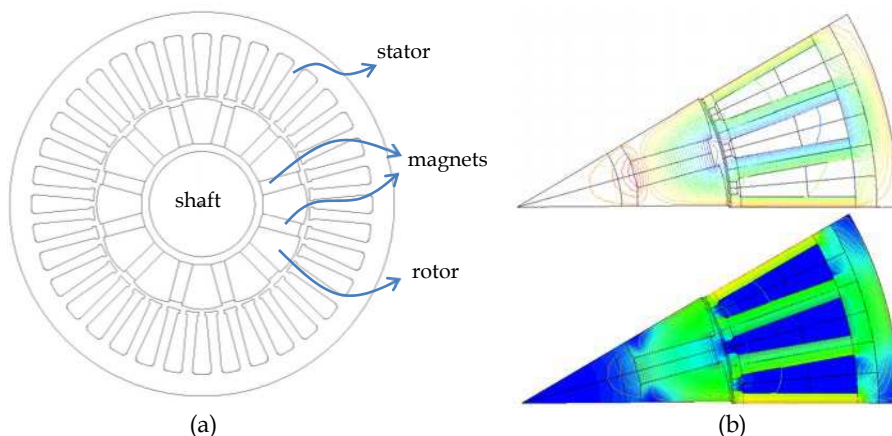


Fig. 18. Spoke type IPM servomotor (a) and flux line and flux distribution (b)

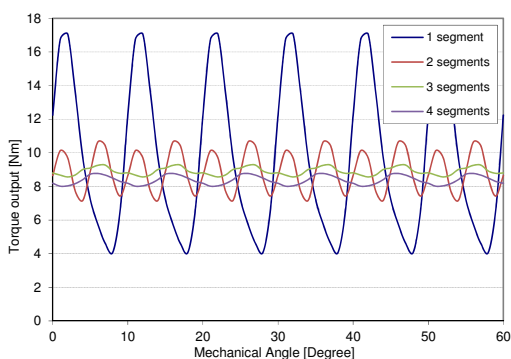


Fig. 19. Torque output variation of the IPM servomotor with low and high torque ripple

8. Control of PM servomotors

Commutation of a brushless pm motor is achieved electronically. Stator winding is energized using an inverter in a sequence. It is crucial to know the position of the rotor so as

to know which winding will be energized. This requires precise information of the rotor position using hall sensors or resolvers. When the rotor magnet poles pass, the position information of the sensor is provided to the controller and inverter drives the motor windings in the correct sequence.

Brushless PM servomotors can have both trapezoidal and sinusoidal back EMF waveforms and are excited with either rectangular or sinusoidal currents. A current regulated voltage source inverter is used to drive the servomotors. Power stage of the converter is combined by a rectifier, DC link and an inverter. Current sensors are used in each phase and fed back to the DSP controller. Position information is frequently obtained either by a resolver or an encoder although hall sensors are preferred for trapezoidal brushless servomotors. The simple system set-up with the main blocks of the system is illustrated in Fig. 20.

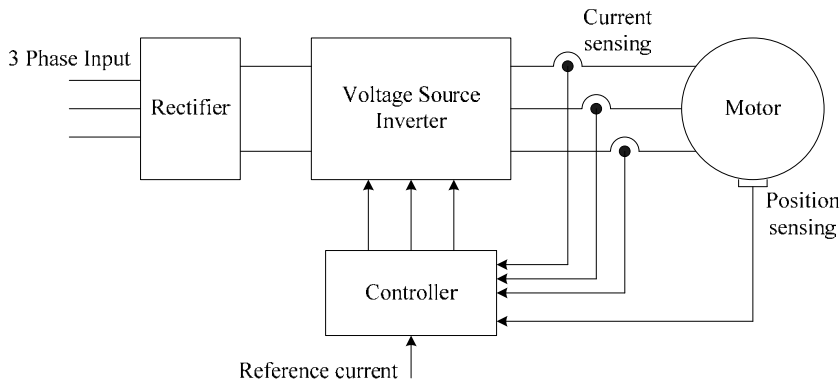


Fig. 20. Permanent magnet servomotor drive

9. Conclusion

Detailed introduction to brushless permanent magnet servomotors used in both industrial and servo applications is provided in this chapter. Motor classification and types, advantages and disadvantages of different PM servomotors and comparison, materials used in motor components are reviewed. Servomotor design process including electromagnetic, structural and thermal steps; softwares used in the analysis, design and optimization of such motors are also enlightened in detail. Torque quality, mathematical output torque equations, cogging and ripple torque components are investigated thoroughly since the torque quality confirms the quality of the servomotor.

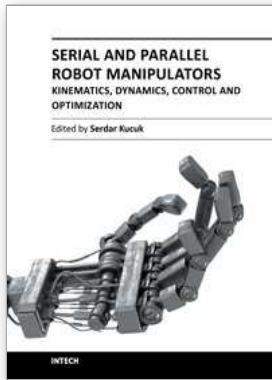
10. Acknowledgment

The authors are indebted to CEDRAT Co. for providing the Flux 2D FEA Package and MDS Motor Ltd. for providing some motor pictures and its facilities in preparing this document.

11. References

Flux 2D and 3D Tutorial, Cedrat Co. 2002.

- J. D. L. Ree and N. Boules, "Torque production in permanent-magnet synchronous motors," *IEEE Trans. Industry Applications*, vol. 25, no. 1, pp. 107-112, 1989.
- J. R. Hendershot and T. J. E. Miller, "Design of Brushless Permanent-Magnet Motors (1995)," Oxford University Press, ISBN 0198593899, UK.
- M. Aydin, M. K. Guven, S. Han, T. M. Jahns and W. L. Soong, "Integrated Design Process and Experimental Verification of a 50 kW Interior Permanent Magnet Synchronous Machine", *17th International Conference on Electrical Machines (ICEM 06)*, Crete, Greece, 2006.
- Motor-CAD v3.1 software manual, April 2006.
- N. Bianchi and S. Bolognani, "Design Techniques for Reducing the Cogging Torque in Surface-Mounted PM Motors", *IEEE Transactions on Industry Applications*, Vol. 38, No. 5, September/October 2002.
- SPEED Software, PC-BDC 9.04 User's Manual, February 2010.
- T. Sebastian, G. R. Slemon and M. A. Rahman, "Design considerations for variable speed permanent magnet motors", *Proceedings of International Conference on Electrical Machines (ICEM) 1986*, pp.1099-1102.
- T.Li, and G. Slemon, "Reduction of cogging torque in PM motors," *IEEE Trans. Magnetics*, vol. 24, no. 6, pp 2901-2903, 1988.
- Thomas M. Jahns and Wen L. Soong, "Pulsating Torque Minimization Techniques for Permanent Magnet AC Motor Drives-A Review", *IEEE Transactions on Industry Applications*, pp. Vol. 43, No. 2, April 1996.



Serial and Parallel Robot Manipulators - Kinematics, Dynamics, Control and Optimization

Edited by Dr. Serdar Kucuk

ISBN 978-953-51-0437-7

Hard cover, 458 pages

Publisher InTech

Published online 30, March, 2012

Published in print edition March, 2012

The robotics is an important part of modern engineering and is related to a group of branches such as electric & electronics, computer, mathematics and mechanism design. The interest in robotics has been steadily increasing during the last decades. This concern has directly impacted the development of the novel theoretical research areas and products. This new book provides information about fundamental topics of serial and parallel manipulators such as kinematics & dynamics modeling, optimization, control algorithms and design strategies. I would like to thank all authors who have contributed the book chapters with their valuable novel ideas and current developments.

How to reference

In order to correctly reference this scholarly work, feel free to copy and paste the following:

Metin Aydin (2012). Brushless Permanent Magnet Servomotors, Serial and Parallel Robot Manipulators - Kinematics, Dynamics, Control and Optimization, Dr. Serdar Kucuk (Ed.), ISBN: 978-953-51-0437-7, InTech, Available from: <http://www.intechopen.com/books/serial-and-parallel-robot-manipulators-kinematics-dynamics-control-and-optimization/brushless-permanent-magnet-servomotors-used-in-manipulators>

INTECH

open science | open minds

InTech Europe

University Campus STeP Ri
Slavka Krautzeka 83/A
51000 Rijeka, Croatia
Phone: +385 (51) 770 447
Fax: +385 (51) 686 166
www.intechopen.com

InTech China

Unit 405, Office Block, Hotel Equatorial Shanghai
No.65, Yan An Road (West), Shanghai, 200040, China
中国上海市延安西路65号上海国际贵都大饭店办公楼405单元
Phone: +86-21-62489820
Fax: +86-21-62489821

© 2012 The Author(s). Licensee IntechOpen. This is an open access article distributed under the terms of the [Creative Commons Attribution 3.0 License](#), which permits unrestricted use, distribution, and reproduction in any medium, provided the original work is properly cited.